Bioorganic & Medicinal Chemistry Letters 20 (2010) 586–590

Contents lists available at ScienceDirect

Bioorganic & Medicinal Chemistry Letters

journal homepage: www.elsevier.com/locate/bmcl

Structure-guided design of α-amino acid-derived Pin1 inhibitors

Andrew J. Potter, Stuart Ray, Louisa Gueritz, Claire L. Nunns, Christopher J. Bryant, Simon F. Scrace, Natalia Matassova, Lisa Baker, Pawel Dokurno, David A. Robinson †, Allan E. Surgenor, Ben Davis, James B. Murray, Christine M. Richardson ‡, Jonathan D. Moore *

Vernalis (R&D) Ltd, Granta Park, Great Abington, Cambridge CB21 6GB, United Kingdom

ARTICLE INFO

Article history:
Received 21 October 2009
Revised 16 November 2009
Accepted 17 November 2009
Available online 22 November 2009

Keywords:
Pin1
Cancer
Rotamase
Isomerase
Kinase signaling
Crystal structure
Small molecule inhibitor
NMR
Surface plasmon resonance

ABSTRACT

The peptidyl prolyl cis/trans isomerase Pin1 is a promising molecular target for anti-cancer therapeutics. Here we report the structure-guided evolution of an indole 2-carboxylic acid fragment hit into a series of α-benzimidazolyl-substituted amino acids. Examples inhibited Pin1 activity with IC_{50} <100 nM, but were inactive on cells. Replacement of the benzimidazole ring with a naphthyl group resulted in a 10–50-fold loss in ligand potency, but these examples downregulated biomarkers of Pin1 activity and blocked proliferation of PC3 cells.

Pin1 provides the great majority of peptidyl prolyl cis/trans isomerise (PPIase) activity capable of isomerising pSer/pThr-Pro bonds.[1] Isomerisation around such bonds can promote major conformational changes within proteins, enabling Pin1 to influence dynamics and outcomes within pathways regulated by MAP kinases, cyclin-dependent kinases and GSK-3β.[2–6] Pin1 overexpression is only weakly oncogenic in itself, but enhances transformation by ErbB2 or activated Ras alleles.[5] Remarkably, cells from Pin1 deficient mice are resistant to transformation by Ras and ErbB2.[7] As Pin1-deficient mice are viable,[8] there are considerable grounds for hope that Pin1 inhibitors will have value for the therapy of cancer.

The irreversible inhibitor, Juglone (**1**), has been widely used to probe the function of Pin1 inside cells, but is neither selective nor a suitable start point for drug discovery.[9–11] Several classes of presumably reversible small molecule inhibitors have since been reported.[12,13]Structural data confirming interactions of inhibitor with Pin1, however, has been restricted to peptide antagonists,[14,15] with the exception of a series of phenylalaninol phosphates, recently disclosed by Pfizer.[16] The same report revealed that when 10^6 compounds were screened for activity against Pin1 no hits were found whose binding to target could be verified by isothermal titration calorimetry or NMR.[16] This suggests high-throughput screening is not an effective way of finding start points for drug discovery programs targeting Pin1, but that alternative approaches should be sought.

Vernalis have developed an NMR-based fragment screening platform (SeeDs) capable of identifying compounds that compete for binding to target with known competitor ligands.[17,18] Two competitor ligands had been identified whose binding to the Pin1 active site had been verified by crystallography: the D-peptide inhibitor **2**, and the phenylalaninol phosphate **3**.[15,16] To identify potential start points for drug discovery, a library of ~1200 fragments was screened by NMR for their ability to compete with the binding of **2** and **3** to the PPIase domain of Pin1. This process identified five competitively-binding compounds,[19] of which the indole 2-carboxylic acid **4** (IC_{50} 16 μM) was the most potent inhibitor of Pin1's PPIase activity.[20]

Pin1 crystals were readily obtained from an R14A (Arg14 mutated to Ala) variant of full length Pin1,[14] or a K77Q/K82Q mutated variant of the isolated peptidyl-prolyl isomerase domain.[16] Compound **4** was soaked into crystals of Pin1R14A protein. This enabled the determination of a ligand-bound X-ray crystal structure (Fig. 1), in which the indole moiety fits snugly into a hydrophobic

* Corresponding author. Tel.: +44 1223 895555.
E-mail address: j.moore@vernalis.com (J.D. Moore).
† Present address: Division of Biological Chemistry & Drug Discovery, College of Life Sciences, James Black Centre, University of Dundee, Dundee DD1 5EH, UK.
‡ Present address: Biofocus DPI, Chesterford Research Park, Saffron Walden, Essex CB10 1XL, UK.

0960-894X/$ - see front matter © 2009 Elsevier Ltd. All rights reserved.
doi:10.1016/j.bmcl.2009.11.090

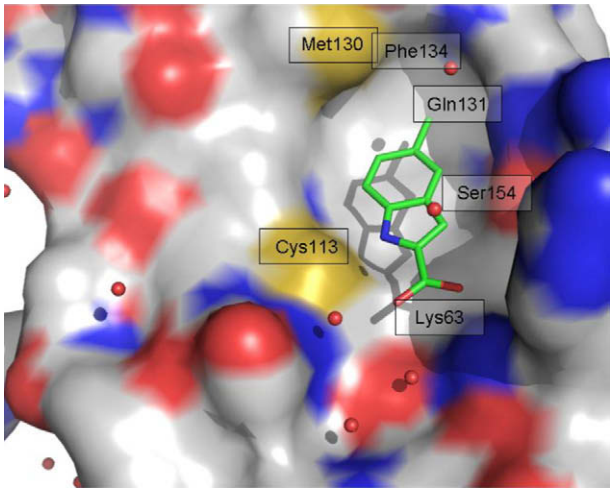

Figure 1. Crystal structure of **4** bound to Pin1R14A (PDB ID: 3KCE). The indole occupies the catalytic site of Pin1. H-bonding interactions (not shown) are observed between the indole nitrogen and cysteine 113 and the indole carboxylic acid to lysine 63. The position of water molecules is shown in red.

pocket in the Pin1 active site. The indole NH hydrogen bonds to the side chain of Cys113, whilst the carboxylic acid substituent interacts with Lys63 and a network of waters.

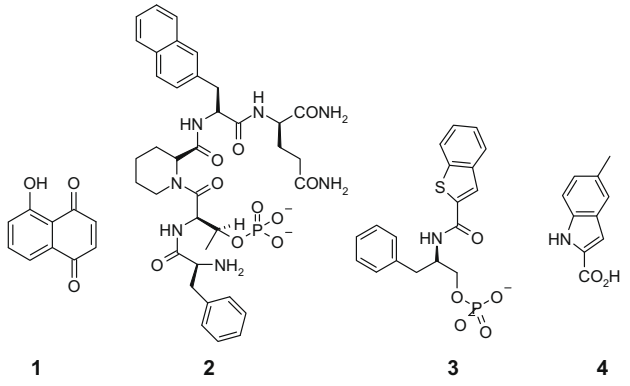

1 **2** **3** **4**

PPIase assay results for **4** (IC_{50} 16 μM) implied a very high ligand efficiency[21] (LE = 0.48). To verify this value, binding affinity was investigated by surface plasmon resonance spectroscopy (SPR). At low ligand concentrations, less **4** bound to Pin1 than expected, but the bound quantity increased rapidly with concentration to super-stoichiometric levels.[20] As binding of **4** to Pin1 could not be saturated, no K_D for the interaction could be calculated. Two-dimensional NMR studies (HSQC), however, showed that shifts in peak positions induced by **4** converged to a maximum value, suggesting a K_D of ~200 μM.[20] Adjusting buffer and salt concentrations in the PPIase assay so as to mimic conditions in the SPR or NMR experiments made no difference to the IC_{50} obtained. The high affinity of the interaction of **4** with Pin1 that would be inferred from the PPIase assay results was therefore not confirmed by biophysical techniques, but **4** nevertheless remained an interesting start point for drug discovery. Possible explanations for these contradictory results are discussed in the Supplementary data.[20]

SAR was investigated amongst several commercially available indole-2-carboxylates. Given the disagreement between the PPIase assay and other techniques, only tentative conclusions regarding ligand activity can made from PPIase assay data alone. Nevertheless, the crystal structure of the 6-methyl substituted compound (**5**) (IC_{50} 630 μM) revealed the position of the methyl substituent was dominant over the indole nitrogen in orientating the molecule in the Pin1 active site.[20] This result indicated that indole NH moieties could hydrogen bond to residues on either side of the active site pocket. To probe SAR in more detail, several benzimidazole 2-carboxylic acids were synthesized (Scheme 1).

Appropriately substituted *o*-phenylene-diamines were condensed (**6**) with 2,2,2-trichloroacetimidic acid methyl ester. Hydrolysis of the intermediate 2-trichloro-benzimidazoles (**7**) yielded the corresponding benzimid-azole 2-carboxylic acids. Compound **8a** (IC_{50} 63 μM), the benzimidazole analogue of **4**, was less active than its indole counterpart (see Table 1). Replacement of the 5-methyl substituent of **8a** with a nitrile (**8b**) increased potency ~7-fold (IC_{50} 10 μM). The interaction between the carboxylic acid group and Lys63 was essential for inhibition: a series of compounds where the acid in **8a** was replaced with amides (e.g., compound **9**) were inactive in the PPIase assay. This demonstrates the importance of the bridging waters seen in the X-ray structure of **4** bound to Pin1.

The phenylalaninol phosphate **3** can be considered to make three points of attachment with Pin1. The phenylalanine moiety fills the hydrophobic pocket, the phosphate hydrogen bonds with Ly63, Arg68 and Arg69, and the thiophene group binds to a 'shelf-like' flat hydrophobic surface located on the other side of Cys113, away from the active site.[16] The indole 2-carboxylic acid fragment hit **4** mimicked the first two of these interactions, and had the potential advantage of not having a phosphate group, which might be expected to interfere with cell penetration. Consequently, we were keen to explore means by which our ligands could be elaborated to access this shelf. Unfortunately, **4** did not present positions for elaboration that provided a suitable vector. Analogue screening identified 3-(1*H*-benzo-imidazol-2-yl)-propionic acid (**10**), which crystallized in the active site in the PPIase K77Q/K82Q form of Pin1 so as to retain the interactions observed for **4**: the fused ring system binding to the hydrophobic pocket and acid participating in a salt bridge with Lys63.[20] Crucially, a vector towards the shelf is available by substitution off the methylene carbon, α to the acid in **10**.[20] Whilst **10** was less active (IC_{50} 740 μM) than **4**, its ligand efficiency (LE = 0.29) was considered acceptable for a start point, given the shallow highly-solvated

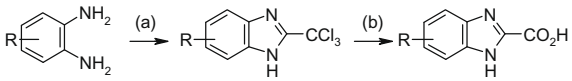

6 **7** **8**

Scheme 1. Reagents and conditions: (a) 2,2,2-trichloroacetimidic acid methyl ester, $MeCO_2H$, 80%; (b) $NaOH_{(aq)}$; $HCl_{(aq)}$, 55–75%.

Table 1
Biological data for indole/benzimidazole Pin1 inhibitors

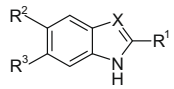

	R^1	R^2	R^3	X	Pin1 IC_{50}[a] (μM)
4	CO_2H	Me	H	C	16
5	CO_2H	H	Me	C	630
8a	CO_2H	Me	H	N	63
8b	CO_2H	CN	H	N	10
9	CONHEt	Me	H	N	>2000
10	$(CH_2)_2CO_2H$	H	H	N	740
11	$(CH_2)_2CO_2H$	H	H	C	450

[a] All IC_{50} values are the mean of at least two determinations and are rounded to two significant figures where appropriate.

Pin1 active site. Compound **11**, the indole analogue of **10**, had similar activity (IC_{50} 440 μM).

Study of the ligand bound crystal structure of **10** suggested a viable way to access the hydrophobic shelf was via elaboration of the 2-position. (*R*)-Amino acid derivatives were of particular interest and the required amides were prepared by the route shown in Scheme 2. The commercially available aspartic acid derivative (**12**) was esterified with potassium carbonate and methyl iodide and the resulting diester (**13**) then hydrogenated using palladium on carbon, yielding the mono acid (**14**) in good overall yield. Benzimidazole formation was achieved through coupling of *o*-phenylenediamine to the mixed anhydride of the mono acid followed by cyclization under acidic conditions to yield **15**. The BOC-protected benzimidazole (**16**) was then de-protected using TFA and coupled to the desired carboxylic acids using carbodiimide/triethylamine. Finally, esters (**17**) were saponified to yield the corresponding acids (**18–20**) on work up. Analysis of these final compounds showed that some degree of racemization had taken place along the synthetic route. Chiral HPLC showed that the *R*-enantiomers were approximately 75% ee.[20]

The propionyl amide **18a** (78 μM) had ~10-fold improved potency over the parent **10**, but the indolyl-propionyl amide **18b** (6 μM) was more active still (Table 2). X-ray crystal structures of these amides were not obtained, but the structure obtained when the phenylpropionyl amide (**18c**) was soaked into crystals of Pin1-R14A/Q131A (a Pin1 variant bearing a mutation facilitating crystallisation with a more open binding site) revealed that the phenyl moiety was positioned on the shelf as expected.[20] The flexibility inherent in the side chains of compounds **18b** and **18c** suggested there would be an entropic penalty to their binding to Pin1, so other, more rigid examples were also prepared. This tactic led to rapid success: the benzothiophene substituted derivative (**18d**) inhibited Pin1 with an IC_{50} <1 μM in the PPIase assay and could also be soaked into crystals of Pin1 R14A/Q131A.[20]

SPR indicated the over-binding phenomenon observed with the earlier fragment was no longer apparent. Binding of **18d** to Pin1 was shown to saturate, with one ligand molecule bound per receptor. The K_D for the interaction was estimated by SPR to be ~10 μM.[20] The structure of **18d** bound to Pin1 suggested that there was an opportunity to improve potency by increasing the area of shelf surface that they covered. The effectiveness of other ring systems linked through the amide was therefore explored. The 2-methylfuran-3-carbonyl amide **19a** was prepared to establish if this moiety would provide a good basis for this exercise. The crystal structure of **19a** in Pin1R14A[20] suggested that further elaboration off the 5-position of the furan would be beneficial, and this resulted in the identification of a superior compound with sub-200 nM potency (**19b**). The substantial potency gain is considered to be associated with good van der Waals contacts between the ligand side chain and shelf, combined with liberation of water molecules otherwise constrained against the hydrophobic ligand and protein surfaces, giving rise to a substantial entropic gain on their displacement back into solvent. The negatively charged carboxylate remains a requirement for activity as **17b**, the methyl ester of **19b**, loses activity by >100-fold. Several 5-phenyl-substituted furan compounds were synthesized and assayed for their ability to inhibit Pin1. These compounds differed only in terms of 4-position substitution off the phenyl ring. The most potent compound, the amino-methyl substituted phenyl derivative **19e** inhibited Pin1 with an IC_{50} of ~20 nM. SPR confirmed a sub-μM K_D (530 nM) for the interaction between **19e** and Pin1 and a 1:1 stoichiometry.[20]

Neither **19b** nor its close relatives could be crystallized in Pin1, but modelling was consistent with a crystal structure subsequently derived for **20**, a 5-phenyl-2-methyl pyrazole substituted compound (IC_{50} 260 nM). In the crystal structure of **20** in Pin1R14A (Fig. 2) the benzimidazole binds as previously observed, though the carboxylic acid group is laterally displaced relative to **10**. On the shelf, the phenyl and pyrazole rings of **20** make good contact with the surface, though the nitrogen of the pyrazole ring does not seem to make direct polar interactions with either protein residues or ordered waters.

Compounds **19b** and **20** were unable to inhibit the PPIase activity of FKBP12 or cyclophilin A, suggesting that they specifically antagonised Pin1. Furthermore, the (*S*)-enantiomers of these two

Table 2
Biological data for benzimidazole propionate Pin1 inhibitors

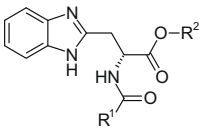

	R^1	R^2	Pin1 IC_{50} (μM)	LE[21]
18a	Et	H	78	0.28
18b	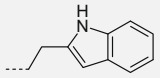	H	6.3	0.24
18c	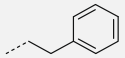	H	7.5	0.26
18d	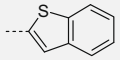	H	0.83	0.30
19a		H	6.6	0.29
19b	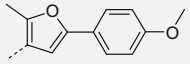	H	0.13	0.29
17b	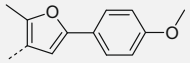	CH_3	92	0.16
19c	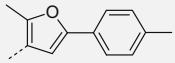	H	0.32	0.28
19d	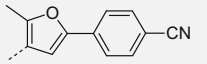	H	0.18	0.28
19e	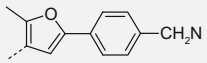	H	0.025	0.32
20	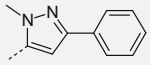	H	0.26	0.29

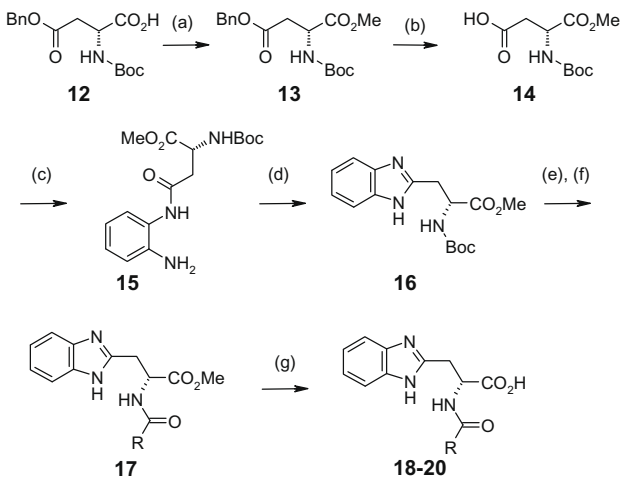

Scheme 2. Reagents and conditions: (a) Na_2CO_3, MeI, DMF, 90%; (b) H_2, Pd/C, MeOH, 100%; (c) IBCF, NEt_3, phenylenediamine; (d) AcOH, 65 °C, 80% over 2 steps; (e) CF_3CO_2H; (f) RCO_2H, EDAC, NEt_3, DMF, 50–60%; (g) LiOH, THF, H_2O, 90–95%.

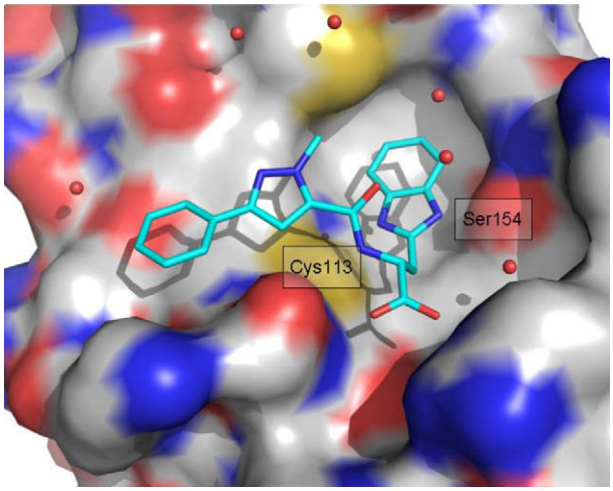

Figure 2. Crystal structures of **20** bound to Pin1R14A (PDB ID: 3KAH). The phenyl pyrazole group makes Van der Walls interactions with the hydrophobic shelf. Incorporation of the benzimidazole achieves a second H-bonding interaction to serine 154.

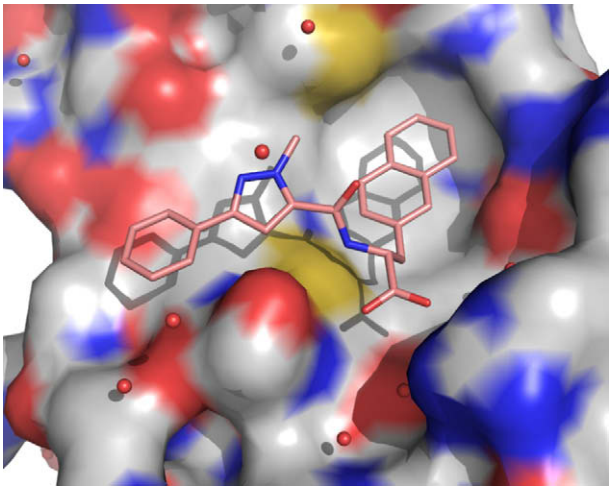

Figure 3. Crystal structure of **23b** bound to Pin1R1 (PDB ID: 3KAI). Replacement of the benzimidazole with naphthyl group does not alter binding mode.

compounds (determined by chiral HPLC to be 100% ee) were inactive in the Pin1 PPIase assay (IC_{50} >10 μM).[19] The more potent benzimidazole-based Pin1 inhibitors were assayed for their ability to inhibit growth of PC3 prostate cancer cells under serum-free conditions where Pin1 plays an important role in survival and proliferation.[22] Unfortunately, none of the compounds were active in cell-based assays, which is consistent with their high polar surface area (PSA) and, where tested, extremely low permeability in CaCo-2 assays (data not shown). To generate Pin1 inhibitors with reduced PSA, the commercially available napthyl alanine derivative (**21**) was coupled to the desired carboxylic acids using carbodiimide/triethylamine and esters (**22**) were saponified to yield the corresponding acids. This resulted in **23a** and **23b**, the napthyl substituted analogues of the benzimidazoles **19b** and **20**, respectively (Scheme 3).

Compound **23b**, the naphthyl-substituted version of **20**, was a less efficient inhibitor of Pin1 (IC_{50} 3.9 μM; LE 0.23) but crystallized in Pin1R14A with a similar binding mode (Fig. 3). Although the acid group is slightly less well-positioned to interact with Lys63, the pyrazolophenyl side chain retains good stacking against the shelf-like hydrophobic surface. The naphthyl ring of **23b** occupies a similar position to the benzimidazole ring of **20**, but protrudes beyond it, packing against the side chains of Phe134, His157, Met130 and Gln131. The similar binding modes of **20** and **23b** imply the >10-fold loss in potency is likely due to loss of H-bond interactions formed by the benzimidazole **20** with Cys113 and Ser154. Encouragingly, **23b**, along with the naphthyl-substituted phenyl furan **23a** (IC_{50} 2.6 μM, LE 0.22) was able to inhibit the growth of PC3 cells under serum-free conditions (Table 3).

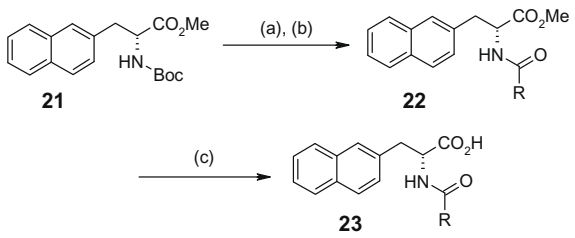

Scheme 3. Reagents and conditions: (a) CF_3CO_2H, (b) RCO_2H, EDAC, NEt_3, 70–75%; (c) LiOH, THF, H_2O, 100%.

Table 3
Biological data for naphthyl-substituted amino acids

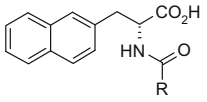

	R	Pin1 IC_{50} (μM)	PC3 GI_{50} (μM)
23a	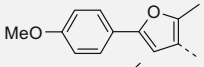	2.6	12.5
23b	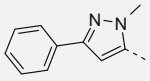	3.9	4.7

For **23a** in particular, good evidence was obtained that its mode of action on cells was, at least in part, via Pin1 inhibition (Fig. 4). In serum starved PC3 cells, **23a** phenocopied transfection of siRNAs versus Pin1 in suppressing cyclin D1 expression (EC_{50} ~ 10 μM) but leaving cyclin E1 levels unaffected. **23a** also prevented the

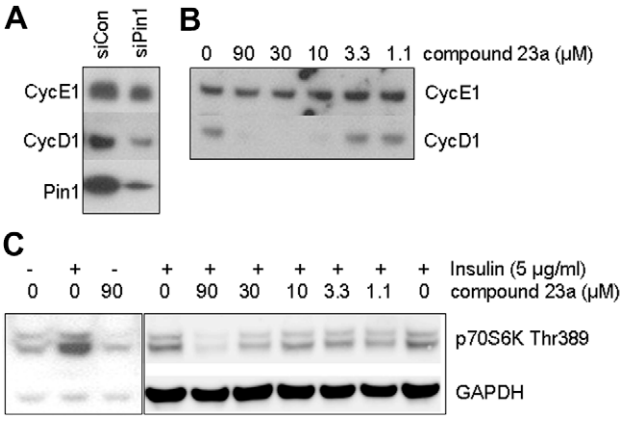

Figure 4. Compound **23a** modulates biomarkers dependent upon Pin1 function. (A) Transfection of siRNA versus Pin1 reduces expression of cyclin D1, but cyclin E1 levels are unaffected. (B) 6 h exposure to **23a** reduces cyclin D1 levels, but cyclin E levels are unaffected. (C) 20 min stimulation with insulin increases phosphorylation of p70S6 kinase on Thr389; this response is blocked by 60 min pre-treatment with **23a**. All data shown is from cells cultured in serum-free conditions for at least 24 h before cells were harvested.

phosphorylation of p70S6 kinase on Thr389 normally induced by insulin[23] ($EC_{50} \sim 30$ μM). Further characterization of **23**a will be reported elsewhere.

In conclusion, this study reports the identification of a fragment hit (**4**) in an NMR-based screen, and then the elaboration of a related fragment (**10**) to compounds with nM potency against Pin1 using a structure-based approach. Cell active compounds (**23a** and **23b**) inhibiting Pin1 in the low μM range were obtained following a further scaffold switch. These results suggest identification of reversible Pin1 inhibitors with properties consistent with their use as drugs may be possible and that structure-guided methods constitute an attractive route towards this goal.

Acknowledgements

We thank Günter Fischer (MPI,Halle, Germany) and Martin Drysdale for useful discussions, Douglas Williamson and Nicolas Foloppe for critical reading of the manuscript and David Bell (Analytical Research and Services, PA, USA) for ee analysis.

Supplementary data

Supplementary data associated with this article can be found, in the online version, at doi:10.1016/j.bmcl.2009.11.090.

References and notes

1. Fanghänel, J.; Akiyama, H.; Uchida, C.; Uchida, T. *FEBS Lett.* **2006**, *580*, 3237.
2. Yaffe, M. B.; Schutkowski, M.; Shen, M.; Zhou, X. Z.; Stukenberg, P. T.; Rahfeld, J. U.; Xu, J.; Kuang, J.; Kirschner, M. W.; Fischer, G.; Cantley, L. C.; Lu, K. P. *Science* **1997**, *278*, 1957.
3. Wulf, G. M.; Ryo, A.; Wulf, G. G.; Lee, S. W.; Niu, T.; Petkova, V.; Lu, K. P. *EMBO J.* **2001**, *20*, 3459.
4. Ryo, A.; Nakamura, M.; Wulf, G.; Liou, Y. C.; Lu, K. P. *Nat. Cell Biol.* **2001**, *3*, 793.
5. Ryo, A.; Liou, Y. C.; Wulf, G.; Nakamura, M.; Lee, S. W.; Lu, K. P. *Mol. Cell. Biol.* **2002**, *22*, 5281.
6. Xu, Y. X.; Hirose, Y.; Zhou, X. Z.; Lu, K. P.; Manley, J. L. *Genes Dev.* **2003**, *17*, 2765.
7. Wulf, G.; Garg, P.; Liou, Y. C.; Iglehart, D.; Lu, K. P. *EMBO J.* **2004**, *23*, 3397.
8. Liou, Y. C.; Ryo, A.; Huang, H. K.; Lu, P. J.; Bronson, R.; Fujimori, F.; Uchida, T.; Hunter, T.; Lu, K. P. *Proc. Natl. Acad. Sci. U.S.A.* **2002**, *99*, 1335.
9. Hennig, L.; Christner, C.; Kipping, M.; Schelbert, B.; Rücknagel, K. P.; Grabley, S.; Küllertz, G.; Fischer, G. *Biochemistry* **1998**, *37*, 5953.
10. Rippmann, J. F.; Hobbie, S.; Daiber, C.; Guilliard, B.; Bauer, M.; Birk, J.; Nar, H.; Garin-Chesa, P.; Rettig, W. J.; Schnapp, A. *Cell Growth Differ.* **2000**, *11*, 409.
11. Fila, C.; Metz, C.; Van der Sluijs, P. *J. Biol. Chem.* **2008**, *283*, 21714.
12. Uchida, T.; Takamiya, M.; Takahashi, M.; Miyashita, H.; Ikeda, H.; Terada, T.; Matsuo, Y.; Shirouzu, M.; Yokoyama, S.; Fujimori, F.; Hunter, T. *Chem. Biol.* **2003**, *101*, 15.
13. Daum, S.; Erdmann, F.; Fischer, G.; Féaux de Lacroix, B.; Hessamian-Alinejad, A.; Houben, S.; Frank, W.; Braun, M. *Angew. Chem., Int. Ed.* **2006**, *45*, 7454.
14. Wildemann, D.; Erdmann, F.; Alvarez, B. H.; Stoller, G.; Zhou, X. Z.; Fanghänel, J.; Schutkowski, M.; Lu, K. P.; Fischer, G. *J. Med. Chem.* **2006**, *49*, 2147.
15. Zhang, Y.; Daum, S.; Wildemann, D.; Zhou, X. Z.; Verdecia, M. A.; Bowman, M. E.; Lücke, C.; Hunter, T.; Lu, K. P.; Fischer, G.; Noel, J. P. *ACS Chem. Biol.* **2007**, *2*, 320.
16. Guo, C.; Hou, X.; Dong, L.; Dagostino, E.; Greasley, S.; Ferre, R. A.; Marakovits, J.; Johnson, M. C.; Matthews, D.; Mroczkowski, B.; Parge, H.; VanArsdale, T.; Popoff, I.; Margosiak, S.; Thomson, J.; Los, G.; Murray, B. W. *Bioorg. Med. Chem. Lett.* **2009**, *19*, 5613.
17. Baurin, N.; Aboul-Ela, F.; Barril, X.; Davis, B.; Drysdale, M.; Dymock, B.; Finch, H.; Fromont, C.; Richardson, C.; Simmonite, H.; Hubbard, R. E. *J. Chem. Inf. Comput. Sci.* **2004**, *44*, 2157.
18. Hubbard, R. E.; Chen, I.-J.; Davis, B.; Drysdale, M. J. *Curr. Top. Med. Chem.* **2007**, *7*, 1568.
19. Data not shown.
20. See Supplementary data.
21. Hopkins, A. L.; Groom, C. R.; Alex, A. *Drug Discovery Today* **2004**, *9*, 430.
22. Ryo, A.; Uemura, H.; Ishiguro, H.; Saitoh, T.; Yamaguchi, A.; Perrem, K.; Kubota, Y.; Lu, K. P.; Aoki, I. *Clin. Cancer Res.* **2005**, *11*, 7523.
23. Lee, N. Y.; Choi, H. K.; Shim, J. H.; Kang, K. W.; Dong, Z.; Choi, H. S. *Carcinogenesis* **2009**, *30*, 671.